Water Research 287 (2025) 124477

Contents lists available at ScienceDirect

Water Research

journal homepage: www.elsevier.com/locate/watres

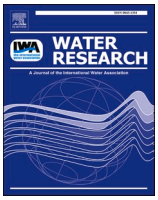

Hybrid regulation of non-conventional water sources powered by renewable energy: advancing circular water management for coastal cities resilience

Miguel-Ángel Bofill [a], Francisco-Javier Sánchez-Romero [b], Francisco A. Zapata [c], Helena M. Ramos [d], Modesto Pérez-Sánchez [a,*]

[a] Hydraulic and Environmental Engineering Department, Universitat Politècnica de València, Valencia 46022 Spain
[b] Rural and Agrifood Engineering Department. Universitat Politècnica de València. Valencia 46022 Spain
[c] Generalitat Valencia Spain
[d] Civil Engineering Research and Innovation for Sustainability (CERIS), Instituto Superior Técnico, Department of Civil Engineering, Architecture and Environment, University of Lisbon 1049-001 Lisbon, Portugal

ARTICLE INFO

Keywords:
Water resources integrated
Water reused
Water resources management
Hybrid water system
Sustainable systems

ABSTRACT

The increasing water scarcity and energy demands in coastal cities, exacerbated by climate variability, necessitate integrated and sustainable water management solutions. This study introduces a novel hybrid volume regulation framework that leverages non-conventional water sources including reclaimed wastewater, stormwater runoff, and desalinated water to achieve circular water use and zero discharge into natural bodies. The aim is the use of non-conventional resources by the integration of hydraulic and energy models through genetic algorithm optimization, enabling the design of a resilient infrastructure to improve the deficit hydric in irrigation communities. Optimal configuration of storage and flow dynamics was defined, ensuring coordinated operation across diverse and spatially distributed sources. The methodology, which is replicable to any case study knowing both hydraulic and energy constraints, shows the design and annual management rule to transfer 17 hm^3. It shows values of capacity ratio, distribution ratio and Benefit/Cost above 0.7, 0.9 and 3.1, respectively, for the optimal solution. The framework also incorporates a comprehensive cost-benefit analysis, accounting for social, environmental, and economic impacts, such as desertification mitigation, employment generation, and CO_2 reduction. The findings highlight the replicability and scalability of the proposed model, offering a robust decision-support tool for water governance and supporting Sustainable Development Goals.

List of Acronyms

ACO	Ant Colony Optimization
AE	Average endowment (4990 m^3/ha)
APAS	Average productivity of the agricultural sector (37717 €/worker)
APOS	Average productivity of another sector (51475 €/worker)
B/C	Cost-benefit ratio
BIE	Benefit increased employment (€/year)
BPI	Benefit Productivity Increase (€/year)
C_{BPI}	Coefficient *BPI* (1.01 €/m^3)
C_{IGB}	Coefficient *IGB* (0.3 €/m^3)
C_{LRI}	Water Price (0.3 €/m^3)
Cf	Configuration. Set of variables (pumped flow, volume of reservoirs and photovoltaic power)
Cf_0	Number of configurations.
$C_{j,defined}$	Defined capacity for reservoir *j* in the simulation (m^3)
CEE	Clean Energy Emission Benefit Generation (€/year)
CO2	Carbon oxide emissions
CR	Capacity Ratio
C_{jsR}	Theoretical capacity required for reservoir *j* in scenario *s* (m^3)
DC	Discharge Cost (€/m^3)
DECR	Distributed Energy Consumption Ratio (kWh/m^3)
DI	Demand Index

* Corresponding author.
E-mail addresses: fcosanro@agf.upv.es (F.-J. Sánchez-Romero), zapata_fra@gva.es (F.A. Zapata), helena.ramos@tecnico.ulisboa.pt (H.M. Ramos), mopesan1@upv.es (M. Pérez-Sánchez).

https://doi.org/10.1016/j.watres.2025.124477
Received 1 May 2025; Received in revised form 23 August 2025; Accepted 25 August 2025
Available online 27 August 2025

DPxx	Tanks
DR	Distribution Ratio
DRB	Desertification Reduction Benefit (€/year)
DTI	Demand transferred index
DVR	Distributed Volume Ratio
Dxx	Delivery system
EAC_s	Annual equivalent cost in scenario *s* (€/year)
EC	Employment coefficient (20.51 jobs/hm^3)
E_{ks}	Energy consumed in *k* photovoltaic energy system in scenario *s* (kWh)
$E_{k,G}$	Total energy generated in k photovoltaic energy system (kWh)
EME	Economic multiplier effect (€/year)
E_{ps}	Energy consumed in *s* scenario for *p* pumping system (kWh)
F	Objective function
F_0	Number of objective functions
FF_{CO_2}	Average CO2 fixation factor (13.2 tCO2/ha)
F_{ME}	Multiplier coefficient effect of growth of the agricultural sector
G	Generation
G_0	Number of generation
G_{CO_2}	CO2 value per energy consumed (404 g CO2/kWh)
GCR	Global Capacity Ratio
GDR	Global Distribution Ratio
GPRS	Global Photovoltaic Self consumption
GVA	Gross Value Added
GVA_{AS}	Gross value added of agriculture in the province (€)
H_{jm}	Piezometric level of reservoir *j* for *m* interval (mw.c.)
H_{pm}	Manometric head of pumping for *m* interval and *p* pumping station (mw.c.)
H_{rm}	Water level of resource *r* in hour *m* (m^3)
i	Each Delivery point
I	Maximum number of Delivery points in the system
IC_{s0}	Initial investment in the year 0 (€)
IGB	Incremental Guarantee Benefit (€/year)
j	Each reservoir considered in the system
J	Maximum number of reservoirs in the system
K	Coefficient that weights the difference between 100% use of renewable energy (project) and the average renewable energy that supplies the Spanish electricity grid
k	Each photovoltaic energy system
k_{RD}	Real discount rate k_{RD}=*0.07*
LR	Leakage rate (0.31)
LRI	Leakage Reduction Improvement (€/year)
m	Each interval hour
MRR	Manometric Regulation Ratio
N	Each alternative analized
N_s	Maximum number of alternatives
n	Each year of study
n_0	Maximum number of years
NAP	Non-Agricultural Proportion (4/5)
OMC_s	Operation and maintenance cost in scenario *s* (€/year)
p	Each pumping station
P	Maximum number of pumping station
PC	Proportion of the total volume distributed that flows through leaking pipelines
P_k	Photovoltaic power to be installed for *k* photovoltaic energy system (MW)
$P_{max,k}$	Maximum Photovoltaic power to be installed for *k* photovoltaic energy system defined in the optimization range (MW)
$P_{min,k}$	Minimum Photovoltaic power to be installed for *k* photovoltaic energy system defined in the optimization range (MW)
PSO	Particle Swarm Optimization
PSR	Photovoltaic Self-consumption ratio
PSxx	Pumped system
PSV	Photovoltaic pumped system
QGIS	Quantum GIS
r	Each resource
RSxx	Reservoir
s	Each of the scenarios studied
$S_{province}$	Total area devoted to agriculture in province (ha)
S_b	Benefited area (ha)
SC_{CO_2}	Social cost CO2 (43 €/tCO_2)
SDGs	Sustainable development goals
t	Hourly interval (h)
T	Lifetime (years) T=25 years.
Q_p	Pumped flow(maximum) for *p* pumping station (m^3/s)
$Q_{max,p}$	Maximum pumped flow for *p* pumping station defined in the optimization range (m^3/s)
$Q_{min,p}$	Minimum pumped flow for *p* pumping station defined in the optimization range (m^3/s)
UGPR	Used Generated Power Ratio (Wp/m^3)
$V_{d_{t,i}}$	Hourly Demanded volume for each delivery point *i* (m^3)
$V_{Desalinated_t}$	Hourly volume from desalination plant
$V_{isT,distributed}$	Theoretical volume distributed for user *i* in scenario *s* (m^3)
$V_{its=1,distributed}$	Theoretical volume distributed for user *i* in scenario 1 in (m^3)
$V_{is,distributed}$	Volume distributed for user *i* in scenario *s* in (m^3)
$V_{isT,distributed}$	Theoretical volume distributed for user *i* in scenario *s* (m^3)
V_j	Volume of reservoir *j* (m^3)
$V_{max,j}$	Maximum Volume of reservoir *j* defined in the optimization range (m^3)
$V_{min,j}$	Minimum Volume of reservoir *j* defined in the optimization range (m^3)
$V_{psT,distributed}$	Theoretical volume transferrer for pumping station *p* in scenario *s* (m^3)
$V_{pts=1,distributed}$	Theoretical volume distributed for pumping station *p* in scenario 1
V_{jm}	Volume distributed in reservoir *j* for *m* interval (m^3)
V_{pm}	Pumped volume for *m* interval for *p* pumping station (m^3)
V_{rm}	resource input volume *r* in hour *m* (m^3)
V_{sNT}	Volume not distributed in irrigation areas and discharged to sea in scenario *s* (m^3)
V_{sT}	Theoretical total volume generated by all resources introduced into the system in scenario *s* (m^3)
$V_{Stormwater_t}$	Hourly volume from stormwater runoff collection point
$V_{WWTP\,t}$	Hourly volume from waterwaste treatment plants (m^3)
UGPR	Used Generated Power Ratio
W_k	Installed solar power in *k* photovoltaic system (W)
WBIB	Water bodies Improvement Benefit (€/year)
WWTPs	Waterwaste treatment plants

1. INTRODUCTION

The rapid growth of urban populations is placing increasing pressure on the provision of essential services (Liang et al., 2023). This trend necessitates consuming substantial natural resources, particularly in terms of food, energy, and water (Eshtawi et al., 2016). As a consequence, logistical operations must expand to meet this demand, further exacerbating society's carbon footprint (Koop et al., 2022). Water, a critical resource for both urban and rural populations, is fundamental to effective sanitation, hygiene, and agricultural production (Dotaniya et al., 2023). In rural areas, water not only supports crop cultivation, which sustains the global food supply, but also plays a key role in stabilizing rural economies and preventing depopulation (Anser et al., 2023).

Addressing these challenges calls for the implementation of sustainable strategies that promote the efficient reuse of resources (Hui et al., 2023). Within this context, water reuse emerges as a crucial

element in improving the evaluation of Sustainable Development Goal 6 (SDG6) (Garcia et al., 2023). By integrating circular economy principles into water management, the reuse of treated wastewater not only reduces pollution in rivers and seas but also offers a sustainable solution for water conservation (Guerra-Rodríguez et al., 2020).

Wastewater Treatment Plants (WWTPs) are typically located in the lowest parts of urban areas to take advantage of gravity-fed sewage systems (Estévez et al., 2025). However, the internal purification processes in WWTPs require substantial energy inputs, ranging from 0.4 to 2.7 kWh/m^3, considering tertiary and/or quaternary treatment to be reused in non-potable uses and irrigation consumption (Trapote et al., 2014). When these plants handle effluents from urban or coastal regions, reusing the treated water for purposes such as irrigation or non-potable urban uses (e.g., street cleaning and park irrigation) demands even more energy, including the need for water to be pumped to overexploited aquifers (Ríos et al., 2023). Alicante or Naples are examples of Mediterranean regions where significant volumes of reclaimed water are repurposed for secondary uses. The reuse of this volume implies the pumping systems to distribute the treated water (Su et al., 2020). Therefore, water-reuse projects must be critically evaluated from economic, technical, and environmental standpoints (Molinos-Senante et al., 2011).

National resource planning on this scale can be enhanced through the development of integrated impact analysis toolkits to reduce the water deficit, combining methodologies for social impact assessment (Quinn et al., 2004). Particularly, Spanish irrigation communities have invested heavily in modernizing their infrastructure, particularly through the adoption of localized irrigation methods (Serra-Wittling et al., 2019). This modernization has revitalized previously neglected agricultural lands, boosting irrigation efficiency (Mercedes Garciaarcia et al., 2022). Nevertheless, several factors—including the expansion of cultivated land, increased water demand due to climate variability, and declining water reserves (such as reduced flow from the Tajo-Segura water transfer during droughts)—have driven these communities to seek alternative water sources (García-Ruiz et al., 2011). For instance, irrigation deficits in Mediterranean areas are projected to rise by approximately 40% (Eekhout et al., 2024). In this context, this proposal called zero-discharge strategy, maximize the use of regenerated wastewater as critical approaches to mitigate growing water scarcity in irrigated agriculture (Christou et al., 2024). These practices enhance the resilience and efficiency of water systems by recovering and reallocating residual flows and drainage water (Ramos and Santos, 2010) . Moreover, integrated water reuse models have demonstrated significant potential to stabilize supply under extreme hydrological variability (Pedrero et al., 2010). Their adoption is increasingly recognized as essential for sustainable water resource management in semi-arid regions . Segura basin where the analyzed case study in this research is located has a structural deficit, as it is the only one whose potential resources cannot cover its water demands (Pedrero et al., 2010). It implies the use of new strategies to introduce new water resources, not only to maximize the efficiency in their distribution using hybrid systems while guarantee the water demands.

This situation highlights the necessity for water governance policies to prioritize cost-effective desalination technologies and wastewater reuse as key strategies for sustainable resource management (Estrela-Segrelles et al., 2024). Reclaimed wastewater, particularly in coastal cities and densely populated areas, often remains underutilized, with excess volumes discharged into rivers or seas. An analysis of water management plans reveals that a substantial portion of this reclaimed water could be redirected for agricultural use. For example, the United Arab Emirates generates 289 hm^3 of treated wastewater annually (Al Hamedi et al., 2023), China treats approximately 12.6 million hm^3 (Qadir and Jones, 2024), and Spain produces 4876 hm^3 annually, with water reuse rates ranging from 0 to 91.38%, depending on the region, and an average reuse rate of 10.91% nationwide (del Villar and García-López, 2023). The low percentage of reused water highlights the urgent need for innovative strategies to introduce additional water resources, particularly in agricultural sectors with high water demands (Mishra et al., 2023).

Advanced algorithms and machine learning play a crucial role in optimizing water resource management (Anjum et al., 2023), predicting demand (Oğuz and Ertuğrul, 2023), and detecting losses or infrastructure failures (Joseph et al., 2023). These tools enable real-time decision-making (Fu et al., 2022), improve monitoring and control of complex networks (Wang et al., 2021), and support the development of digital twins to simulate system behaviour (Wu et al., 2023), optimizing operations and maintenance. This leads to better resource utilization, cost savings, and enhanced environmental sustainability in water distribution systems (Xiang et al., 2021). Emerging intelligent optimization algorithms, especially those based on swarm intelligence, offer novel solutions for these systems. Popular techniques include Ant Colony Optimization (ACO) (Zhan et al., 2022) and Particle Swarm Optimization (PSO) (Nishanth et al., 2023), among others reviewed by (Elseify et al., 2024). These methods leverage decentralized decision-making processes to address complex optimization challenges in water distribution (Wang et al., 2023).

This study pioneers the optimization of a zero-discharge water management system by leveraging genetic algorithms within a novel multi-objective framework. A unique contribution of this work is the development of an objective function that holistically integrates economic efficiency, regulatory compliance, and full reuse of water from multiple source, including treated wastewater, rainfall-runoff, and desalinated seawater. A core innovation lies in the integration of these diverse water resources into a decentralized system powered by renewable energy, minimizing environmental impact and enhancing the adaptability and resilience of the infrastructure. This decentralized configuration not only reduces the carbon footprint but also ensures scalability and replicability across various hydraulic and territorial contexts.

The use of genetic algorithms enables the simultaneous optimization of technical, environmental, and social criteria in the design and operation of pumping and distribution systems. This advanced optimization approach supports the development of efficient, low-carbon, and context-adaptive infrastructure. By combining cutting-edge computational methods with principles of circularity and sustainability, the proposed methodology delivers a transformative contribution to integrated water resource management. It directly supports the achievement of the United Nations Sustainable Development Goals, particularly SDG 6 (Clean Water and Sanitation), SDG 9 (Industry, Innovation, and Infrastructure), and SDG 12 (Responsible Consumption and Production).

2. MATERIALS AND METHODS

The proposed methodology is divided into two blocks, each containing different steps, as illustrated in Fig 1. The procedure needs different inputs and iterative methods to establish the infrastructure sizing and energy requirements to supply the water irrigation demand according to water resources and existing volume. The proposed methodology evaluates the available water resources and water needs and proposes different alternatives and scenarios for water resource distribution, and it optimizes the infrastructure necessary to achieve this goal.

2.1. Methodology. Optimization stages

Figure 1 shows the different main steps to define the optimized strategy, segmented into two different phases called “Block A. Evaluation of water resources” and “Block B System optimization”.

- Block A. Evaluation of water resources

The first stage involves a comprehensive quantitative and qualitative assessment of both available water resources and agricultural demands.

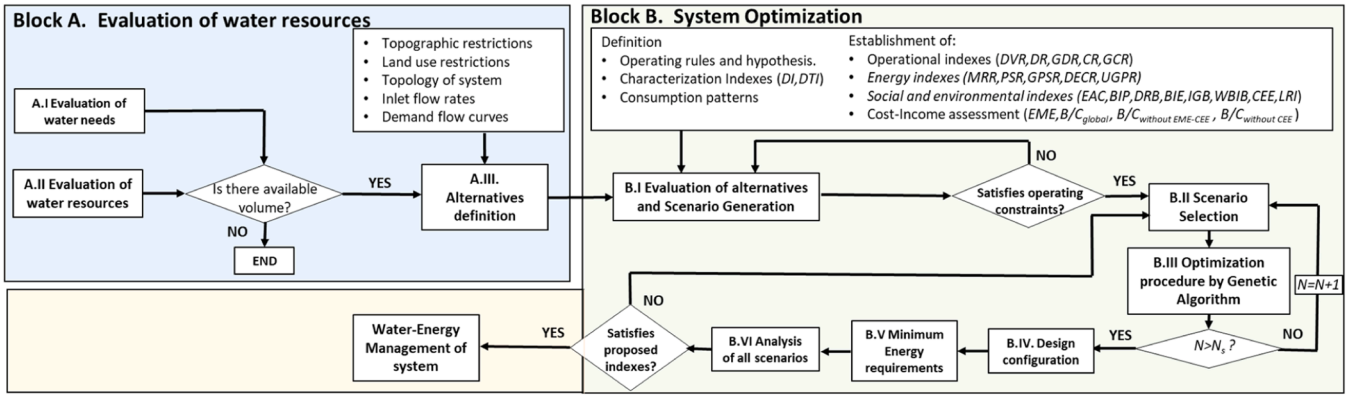

Fig. 1. (a) Proposal of the methodology.

In Step A.I, irrigation requirements are established, along with the water quality standards necessary to meet those demands. This includes identifying rural areas with ongoing agricultural activities that could benefit from the integration of alternative water sources into their existing irrigation systems.

In Step A.II, the potential new water sources are quantified, taking into account their quality, volume, and temporal availability. Water quality is evaluated based on the type of treatment or desalination applied, as well as land characteristics—particularly important when considering runoff generated by rainfall events.

Step A.III If there is the possibility of introducing this volume, a basic model of the system is defined, which allows the evaluation of the essential aspects of the system, including the topology, land use restrictions and topography of the system. The consumption patterns of the irrigation systems and the inflow curves of the resources allow the preliminary determination of the minimum levels and volumes in the reservoirs, and the minimum requirements to ensure the necessary flow and pressure at the consumption points. The reservoirs considered are not conventional dammed reservoirs that collect surface water from rivers or streams within the basin. Instead, they are artificially constructed off-stream storage facilities designed to regulate volumes from various sources. Therefore, they are classified as balancing ponds rather than traditional reservoirs and cannot include the conventional water source analysis of a river. As the methodology is replicable for any case study, if there are water resources from a river, the input should be considered.

This preliminary model offers a robust framework for evaluating multiple feasible alternatives, each defined by critical criteria such as optimal reservoir locations, maintaining minimum piezometric levels, and precise volume regulation. The integration of QGIS routines allows for the strategic identification of reservoir zones, power generation systems, pumping stations, pipeline layouts, and delivery points, facilitating a comprehensive design process. The foundational model is synthesized and validated using the advanced capabilities of EPANET software, ensuring a high level of precision and adaptability.

Any alternative should guarantee the mass balance, which is defined by the following expression:

$$\sum_{t=1}^{8760} V_{d_{t,i}} = \sum_{t=1}^{8760} V_{WWTP_t} + \sum_{t=1}^{8760} V_{Desalinated_t} + \sum_{t=1}^{8760} V_{Stormwater_t} \quad (1)$$

Where $V_{d_{t,i}}$ is the hourly (t) demanded volume for each delivery point (i), V_{WWTP_t} is the hourly volume from waterwaste treatment plants; $V_{Desalinated_t}$ is the hourly volume from desalination plant, and $V_{Stormwater_t}$ is the hourly volume from stormwater runoff collection point. All volumes are considered in m^3.

The different scenarios account for potential variations in water volumes from multiple sources, reflecting the inherent uncertainty associated with annual availability. These variations arise from fluctuations in the volumes of transferred, desalinated, reclaimed (treated wastewater), or rainwater. Consequently, the subsequent optimization phase must ensure a proper distribution of these volumes, considering the randomness in their occurrence. The values are constrained within predefined ranges, established according to existing water rights, concessions, and/or infrastructure capacities. The ratio of each source between the total volume from source enable the definition of the percentage of water coming from each alternative source in the different scenarios analyzed by methodology.

- Block B. System Optimization

Block B contains the main optimization module. The evaluation of alternatives (Step B.I) is established using different indexes, which are focused on hydraulic, energy, economic and environmental values to compare different alternatives and know the real behavior of the system. Multiple demand scenarios are generated for each alternative. Each scenario allows the evaluation of different demand variation hypotheses. These scenarios take into account different demanded volumes and different consumption patterns of users. The objective of analyzing multiple scenarios is to develop operating situations that take into account the variation of the demand curve between consumption users, as well as the volumes demanded. The characterization of the scenarios is done by defining two indexes called the Demand Index (*DI*) and the Demand Transferred Index (*DTI*).

The Demand Index (*DI*) for *s* scenario is defined as the ratio between the theoretical volume distributed and the theoretical volume distributed for scenario number 1. Scenario number 1 is considered the base scenario, with the minimum theoretical volume distributed. The values for *DI* are always equal to or greater than 1 and the maximum value depends on the simulated scenario.

$$DI_s(-) = \frac{\sum_{i=1}^{I} V_{isT,distributed}}{\sum_{i=1}^{I} V_{its=1,distributed}} \quad (2)$$

where $V_{isT,distributed}$ theoretical volume distributed for user *i* in scenario *s* in m^3; $V_{its=1,distributed}$ theoretical volume distributed for user *i* in scenario 1 in m^3.

Demand Transferred Index (DTI) is defined as the ratio between the theoretical volume of water transferred from lower to upper reservoirs in a given scenario and the corresponding volume in Scenario 1. Scenario 1 serves as the baseline, representing the minimum theoretical transfer volume. The *DTI* quantifies the relative increase in the amount of water that must be pumped from lower to upper reservoirs across different scenarios. By definition, the DTI is always greater than or equal to 1, with its maximum value determined by the specific conditions of each simulated scenario.

$$DTI_s(-) = \frac{\sum_{p=1}^{P} V_{psT,distributed}}{\sum_{p=1}^{P} V_{pts=1,distributed}} \quad (3)$$

where $V_{psT,distributed}$ theoretical volume transferrer for pumping station p in scenario s in m^3; $V_{pts=1,distributed}$ theoretical volume distributed for pumping station p in scenario 1 in m^3.

The average of the demand index and the demand transferred index is defined as the supplied volume index, which is used to evaluate the management of the system as well as the satisfaction of its constraints and requirements. The generation of scenarios is based on combinations of different values of the demand index and the demand transferred index, considering the conditions of system management and user requirements. To analyze and compare the system's response across different alternatives and scenarios, several indices are used. The following are defined as operational indices: Distributed Volume Ratio (DVR), Distribution Ratio (DR), and Capacity Ratio (CR).

Distributed Volume Ratio (*DVR*): The purpose of this index is to determine the volume that could not be distributed by the system and has been returned to the sea or not produced. It can oscillate between 0 and 1. The best value is 1.

$$DVR_s = 1 - \frac{V_{sNT}}{V_{sT}} \quad (4)$$

where V_{sNT} is the volume not distributed in irrigation areas and discharged to sea in scenario s in m^3; V_{sT} is the theoretical total volume generated by all resources introduced into the system in scenario s in m^3.

Distribution Ratio (*DR*): This index evaluates the capacity of the volume distribution system according to the established demand curves. This index measures the degree to which the demands of the users have been satisfied. The index is defined as the ratio between the volume that has been distributed to users ($V_{is,distributed}$) and the volume that theoretically should have been distributed ($V_{isT,distributed}$). It takes values between 0 and 1, with the ideal value being 1 because it guarantees that all the demand is supplied. It is defined as:

$$DR_s = \frac{V_{is,distributed}}{V_{isT,distributed}} \quad (5)$$

where $V_{is,distributed}$ is the volume distributed for user i in scenario s in m^3; $V_{isT,distributed}$ is the theoretical volume distributed for user i in scenario s in m^3.

This index is defined for each one of the demand points, and when all the demands are considered the Global Distribution Ratio (*GDR*) can be defined as follows:

$$GDR_s = \frac{\sum_{i=1}^{I} V_{is,distributed}}{\sum_{i=1}^{I} V_{isT,distributed}} \quad (6)$$

Capacity Ratio (*CR*): This index is the ratio between the necessary capacity required and the capacity considered in the reservoirs. The purpose of this index is to determine whether the reservoirs defined in the system are oversized. The range is from 0 to 1. Values near zero suggest that the reservoir being studied is oversized, while values near one indicate that it is optimized for regulation in the analyzed scenarios. The Capacity Ratio is a technical index for each reservoir j in scenario s and it is defined as follows:

$$CR_{js} = \frac{C_{jsR}}{C_{j,defined}} \quad (7)$$

where C_{jsR} is the necessary capacity required for reservoir j in scenario s in m^3; $C_{j,defined}$ defined capacity for reservoir j in simulation in m^3.

The procedure is defined as the global capacity ratio (*GCR*) when all reservoirs are considered, showing whether the capacity of the system is undersized or oversized.

$$GCR_s = \frac{\sum_{j=1}^{J} C_{jsR}}{\sum_{j=1}^{J} C_{j,defined}} \quad (8)$$

The system design must guarantee the operation, minimizing energy. To analyze this aspect, the use of different energy indexes is defined as:

Manometric Regulation Ratio (*MRR*) is the ratio between the pumped volume and the distributed and resource input volume. It takes a positive value, being in ideal conditions equal to 1. If there are different pumped units, the value is always above 1. The closest values indicate that less energy is required in the system.

$$MRR_s(-) = \frac{\sum_{m=1}^{8760}\sum_{p=1}^{P} H_{pm}V_{pm}}{\sum_{m=1}^{8760}\left(\sum_{j=1}^{J} H_{jm}V_{jm} - \sum_{r=1}^{R} H_{rm}V_{rm}\right)} \quad (9)$$

where p is each of the pumping stations; H_{pm} is the manometric head of pumping in each hour m in m w.c.; V_{pm} is the volume pumped in hour m in m^3; H_{jm} is the water level of reservoir j in hour m in m^3; V_{jm} is the volume distributed in reservoir j in hour m in m^3; H_{rm} is the water level of resource r in hour m in m^3; V_{rm} is the resource input volume r in hour m in m^3.

Photovoltaic Self-consumption ratio (*PSR*): This index establishes for each energy generation system (k) the ratio between the energy consumed and the total energy generated.

$$PSR_{sk}(-) = \frac{E_{ks}}{E_{k,G}} \quad (10)$$

Where $E_{ks}$is the energy consumed in k photovoltaic energy system in scenario s in kWh; $E_{k,G}$ is the total energy generated in k photovoltaic energy system in kWh. When this index is applied all photovoltaic energy system Global Photovoltaic Self-consumption ratio is defined:

$$GPSR_s(-) = \frac{\sum_{k=1}^{K} E_{ks}}{\sum_{k=1}^{K} E_{k,G}} \quad (11)$$

-Distributed Energy Consumption Ratio (*DECR*). It establishes the ratio between the energy consumed and the volume distributed for each scenario. It is defined as the following expression:

$$DECR_s\left(\frac{kWh}{m^3}\right) = \frac{\sum_{p=1}^{P} E_{ps}}{\sum_{i=1}^{I} V_{is,distributed}} \quad (12)$$

Used Generated Power Ratio (*UGPR*). This index defines the relationship between total installed power for all photovoltaic systems and the volume distributed by the system for each scenario

$$UGPR_s\left(\frac{Wp}{m^3}\right) = \frac{\sum_{k=1}^{K} W_k}{\sum_{i=1}^{I} V_{is,distributed}} \quad (13)$$

where W_k is installed solar power in k photovoltaic system in vatios (W).

To assess the proposal's advantages and disadvantages, environmental, social, and investment factors are considered. A sustainability-focused cost-benefit analysis converts diverse impact metrics into monetary values for meaningful comparison (Borrego-Marín and Berbel, 2019). Table 1 shows the indicators associated with social and environmental impacts.

The indicators to evaluate the direct and indirect results associated with the proposed methodology are:

Investment and maintenance costs (*EAC*): This indicator defines de operating costs of water infrastructure investments. The initial investment includes the cost of the infrastructure and the annual maintenance cost associated with technical and administrative staff and services. This annual equivalent cost can be established by the following expression (Borrego-Marín and Berbel, 2019):

$$EAC_s\left(\frac{€}{year}\right) = \frac{r(1+k_{RD})^T}{(1+k_{RD})^T - 1} IC_{s0} + OMC_s \quad (14)$$

Table 1
Social and environmental evaluation.

Social and Environmental Impact	Direct Impact	Indicator	Indirect Result
Cost Increase	Investment and Maintenance Cost	Investment and Maintenance Cost (EAC)	Funding Costs
Land use in rural areas	Productivity Growth	Benefit Productivity Increase (BPI)	Direct impact and multiplied Gross Valued Added (GVA) effect
	Reduction of desertification	Desertification Reduction Benefit (DRB)	Improving Environmental Sustainability CO2 Capture and Increased Value Added
	Increasing employment	Benefit increased employment (BIE) Incremental Guarantee Benefit (IGB)	Direct and Multiplier Impact
Groundwater reduction Adjustment for reduction inter-basin transfers	Increase in Resources	Water Bodies Improvement Benefit (WBIB)	Increasing the guarantee
Reduction of discharges to watercourses	Discharges of water bodies into watercourses/ seas		Improvement of water bodies
Renewable energies	CO2 emissions	Clean Energy Emission Benefit Generation (CEE)	Reduction of CO2 emissions
Facilities improvement	Leakage reduction	Leakage Reduction Improvement (LRI)	Increased efficiency

where T is the number of years, considering 25 years (Alyssa Ahmad Affandi et al., 2024); k_{RD} is the real discount rate, considering 4% (Migo-Sumagang et al., 2023); IC_{s0} is the investment costs in scenario s in €; OMC_s is the operation and maintenance costs in scenario s in €/year.

When the distributed volume is considere, the distribution cost (DC) can be defined as the following expression:

$$DC\left(\frac{€}{year\ m^3}\right) = \frac{EAC_s\left(\frac{€}{year}\right)}{\sum_{i=1}^{I} V_{is,distributed}(m^3)} \tag{15}$$

Benefit Productivity Increase (*BPI*): Localized irrigation systems improve water use efficiency and crop value-added, increasing the productivity of the irrigated area. *BIP* is defined by the following expression (Expósito and Berbel, 2017):

$$BPI_s\left(\frac{€}{year}\right) = C_{BPI} \sum_{i=1}^{I} V_{is,distributed} \tag{16}$$

where C_{BPI} is the coefficient *BPI*. In the study area the C_{BPI} coefficient is equal to 1.01€/m^3 according to (Segura, 2021).

Desertification Reduction Benefit (*DRB*): The reduction of desertification is associated with the maintenance of cultivated areas and the capture of CO2 associated with their cultivation. Furthermore, the incorporation of these new resources allows for the reduction of groundwater extraction, as well as water transfers from other basins. The *DRB* index establishes the social benefit of CO2 fixation by maintaining the irrigated area. *DRB* can be determined as follows:

$$DRB_s\left(\frac{€}{year}\right) = FF_{CO_2} \frac{\sum_{i=1}^{I} V_{is,distributed}}{AE}\ SC_{CO_2} \tag{17}$$

where FF_{CO_2} is the average CO2 fixation factor established for the typical crops in the study area (vegetables, citrus and stone fruit trees) in 13.2 tCO_2/ha (Bernardo et al., 2020); *AE* average endowment is defined in the different management plans in m^3/ha in this case 4990 m^3/ha; SC_{CO_2} is the social cost equal to 43 €/ tCO2 (Metcalf and Stock, 2017).

Benefit Increased Employment (*BIE*): Increasing the guarantee of supply of water resources and reducing the uncertainty of access to them maintains agricultural activity. The *BIE* is established by the expression:

$$BIE_s\left(\frac{€}{year}\right) = EC \sum_{i=1}^{I} V_{is,distributed}\ (NAP\ APAS + (1 - NAP)APOS) \tag{18}$$

where *EC* is the employment multiplier coefficient considering 20.51 jobs/hm^3 (Segura, 2021); *APAS* is the average productivity of the agricultural sector, considered 37717 €/worker; *APOS* is the average productivity of another sector, considered 51475 €/worker; (Alimentación, 2023) *NAP* Non-Agricultural Proportion, equal 4/5 (Sindicato Central de Regantes del Acueducto 2020).

Incremental Guarantee Benefit (*IGB*): The introduction of water volumes in the system allows the system managers and associated entities to plan medium and long-term action plans. The increase in the guarantee of supply allows the system to generate income from the value of its sale.

$$IGB_s\left(\frac{€}{year}\right) = C_{IGB} \sum_{i=1}^{I} V_{is,distributed} \tag{19}$$

where C_{IGB} is the coefficient *IGB*, in this case, an average price of 0.3 €/m^3 is considered, although depending on the origin of the resource, water prices in the study area differ.

Water bodies Improvement Benefit (*WBIB*): The incorporation of these new superficial resources reduces groundwater extraction and reduces the transfer of volumes from other basins, such as the Tajo-Segura. Groundwater quality is improved. The cost of the price of water derived from the discharge of reused water into the sea, river or natural areas is evaluated using the cost of the water price derived from the discharge of reclaimed water into the sea, river or natural areas. Therefore, the benefit is established according to the expression:

$$WBIB_s\left(\frac{€}{year}\right) = DC \sum_{i=1}^{I} V_{is,distributed} \tag{20}$$

Where *DC* is the discharge cost by destination. In this case, 0.1 €/m^3 and 0.7 €/m^3 are considered for discharges into the sea or river, respectively (Cost et al., 2016).

Clean Energy Emission Benefit Generation (*CEE*): This indicator refers to the social benefit of not generating CO2 with the energy consumed by the system. The following expression allows the calculation of *CEE*.

$$CEE_s\left(\frac{€}{year}\right) = KG_{CO_2} SC_{CO_2} \sum_{p=1}^{P} E_{ps} \tag{21}$$

where K is the coefficient that weights the difference between 100% use of renewable energy (project) and the average renewable energy that supplies the Spanish electricity grid, which corresponds to 50% (Electrica, 2002). In this study, K=0.5; G_{CO_2} is the CO2 value per energy consumed, 404 gCO2/kWh and SC_{CO_2} is the social cost equal to 43€/kgCO2 (Sheet, 2016).

Leakage Reduction Improvement (*LRI*): The replacement of obsolete infrastructure, characterized by a high percentage of leaks primarily caused by pipe failures, enhances system management by enabling the full utilization of available resources and significantly reducing water and energy losses. Water leakage not only leads to a decline in system productivity but also compromises supply reliability. In this context, the benefits associated with leakage reduction are quantified as follows:

$$LRI_s\left(\frac{€}{year}\right) = C_{LRI}\ LR\ PC \sum_{i=1}^{I} V_{is,distributed} \tag{22}$$

Where C_{LRI} is the water price. This value is considered the same value average price of water (C_{IGB}) 0.3 €/m^3; LR is the leakage rate considering an estimated average value equal to 0.31 (Ávila et al., 2021);PC proportion of the total volume distributed that flows through leaking pipelines.

The cost-benefit ratio (B/C) establishes the relationship between the benefits obtained and the costs required. The cost-benefit ratio is defined as:

$$\left(\frac{B}{C}\right)_s(-) = \frac{\sum Beneficits_s + EME}{EAC_s} \tag{23}$$

where $\sum Benefits$ is the sum of all profits obtained in €/year.

$$\sum Benefits = BPI_s + DRB_s + BIE_s + IGB_s + WBIB_s + CEE_s + LRI_s \tag{24}$$

EME is the Economic multiplier effect. This index takes into account the multiplier effect produced by the agricultural sector on the rest of the sectors. This economic multiplier effect is defined by the expression:

$$EME\left(\frac{€}{year}\right) = F_{ME}\ SR\ GVA_{AS} \tag{25}$$

where F_{ME} is the multiplier effect coefficient that takes into account the effect on non-agricultural sectors of the increase of the agricultural Gross Value Added (GVA) by 1€. In this study the value used is 0.49 (Ahluwalia et al., 2021), which was considered in the evaluation of irrigation modernization (Borrego-Marín and Berbel, 2019); SR Surface ratio of benefited area (S_b) to the total area devoted to agriculture in the province ($S_{province}$), in this study $S_b = 10000\ ha$ and $S_{province} = 184243.3\ ha$ and $SR = 0.054$; GVA_{AS} corresponds to the Gross Valued Added of agriculture in the province, in this case $GVA_{AS} = 657106\ €$ (Sindicato Central de Regantes del Acueducto 2020).

Three different values for cost-benefit ratio *(B/C)* are considered: (i) $(B/C)_1$, global *B/C*. It considers all defined indexes previously; (ii) $(B/C)_2$, *B/C* without *EME* and *CEE* defined as minimum *B/C*. It considers the real impact of the water resources management strategy, without considering the economic multiplier effect (*EME*) and the positive impact of the use of clean energies (*CEE*); (iii) $(B/C)_3$, *B/C without CEE*. This indicator estimates the impact of the proposal without considering the positive effect of the use of renewable energies. In all cases, its value is greater than 1 to consider the proposal as viable.

Step B.II. The total number of scenarios can be considerable, so a sample of scenarios is selected to encompass the global behavior of the system and its response to extreme situations of operation. The selected scenarios are optimized in Step B.III (Figure 2).

During this stage, the methodology defines the key parameters required for simulation. This includes specifying the number of generations, the number of individuals per generation, and the criteria for selection, crossover, and mutation. The optimization process supports multiple objective functions and considers several decision variables. In this study, three variable types are optimized: pumped flow, reservoir volume, and the capacity of photovoltaic power to be installed. The configuration values for the simulations are selected within predefined ranges. A real-coded genetic algorithm is employed for encoding the configurations, as this approach offers notable advantages over binary encoding such as improved precision, faster computation, reduced bit requirements, and enhanced exploration of the solution space (Mei and Huang;, 2002). To select only viable configurations, some restrictions are imposed. To improve the selection procedure of individuals in the first generation, lax constraint values are set, and as the number of generations' increases, these values become more restrictive. In this case, to ensure system operation, the indexes (Distribution Volume Ratio –*DVR*-, Global Distributed Ratio -*GDR*, Global Photovoltaic Self consumption Ratio -*GPSR,* and Global Capacity Ratio -*GCR*) are used as restrictions to the generated configurations or solutions.

In the first generation (Step B.III.3), C_{f0} configurations with random values are generated. Subsequent generations are generated following the procedures of genetic algorithms (selection, crossover, and mutation).

The proposed algorithm simulates each generated configuration according to the scheme in Figure 3 (Step III.4). The phase defines the operating conditions of pumping stations, reservoir levels, and maximum pipeline flows. The annual simulation computes hourly demand and pumping flows, along with variations in reservoir volumes and water levels. The iterative annual computation continues until the system is stable, minimizing discrepancies in volume and level while ensuring compliance with mass and energy balance principles.

The algorithm then evaluates the Distribution Volume Ratio (*DVR)*, Global Distributed Ratio (*GDR)*, Global Photovoltaic Self-consumption Ratio (*GPSR),* and Global Capacity Ratio (*GCR)* indexes to assess the feasibility of each configuration. Feasible configurations are stored for further analysis, and the most optimal ones are selected based on the objective function, while non-compliant configurations are discarded.

The evolutionary process initiates with the selection of viable configurations to form the subsequent generation (Step B.III.5). This selection is guided by the optimization objective function, favoring the most promising individuals while preserving a degree of stochasticity to ensure exploratory potential. A subset of these optimal configurations is randomly chosen to undergo genetic crossover. During this stage, pairs of parent configurations are selected, and a crossover point is randomly defined. Genes (i.e., variable values) from one parent are inherited up to

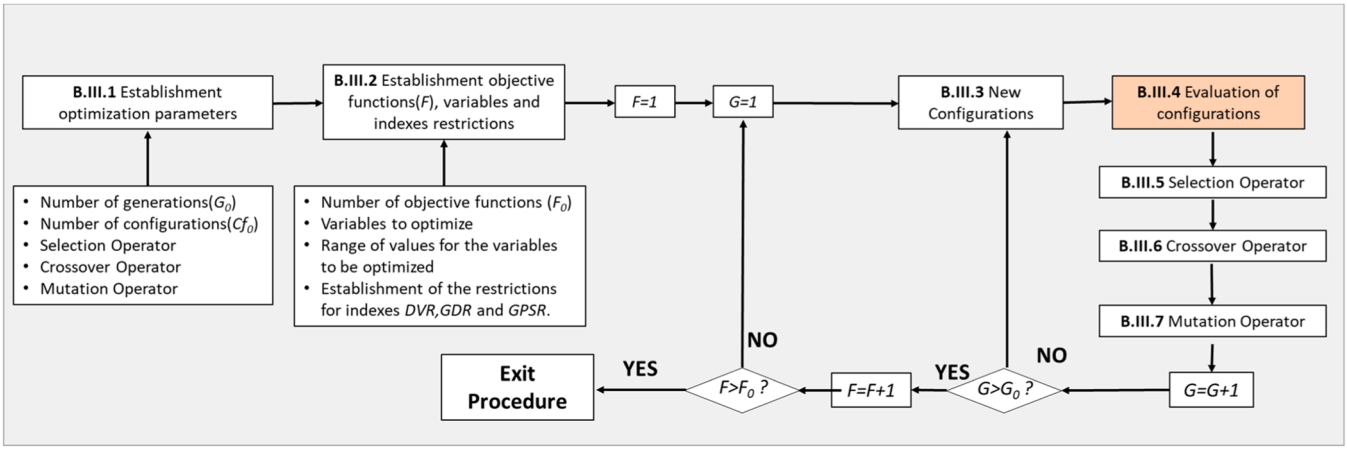

Fig. 2. Block III Optimization procedure by Genetic Algorithm for each selected scenario.

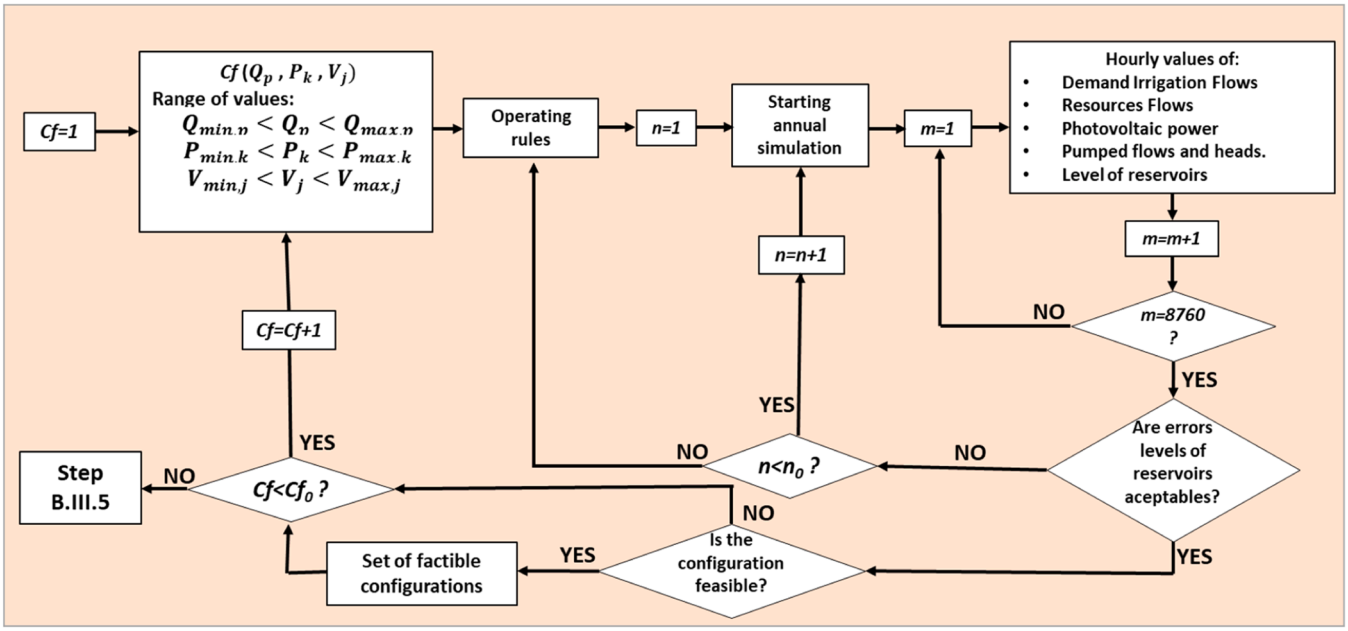

Fig. 3. Evaluation of the configuration in step B.III.4 Block A. Evaluation of water resources.

this point, while the remaining genes are sourced from the second parent. This recombination process is repeated until the target number of offspring configurations is produced.

To safeguard genetic diversity and avoid premature convergence, a mutation operator is applied. Each variable within a configuration is subjected to a mutation probability: if a randomly generated number falls below the specified mutation rate, the variable is perturbed. This introduces novel traits into the population, enhancing the algorithm's ability to explore the solution space.

The resulting generation is composed of configurations derived from crossover, selectively mutated elite individuals, and, optionally, newly introduced random configurations to further diversify the search domain. This iterative evolutionary cycle continues until a predefined maximum number of generations is reached. Upon completion, the subroutine concludes with the evaluation of all objective functions, yielding a robust approximation of the global optimum.

Step B.IV defines the optimal configurations for each objective function, scenario, and alternative. A design configuration is generated, wherein: (i) the geometric characteristics of the reservoirs are refined to align with the constraints of the selected locations, ensuring accurate geometric specifications; and (ii) to minimize energy consumption in the pumping stations, the most suitable machine groups are selected (Step B. V). This selection is further refined through an iterative optimization process based on the Newton-Raphson method (Tsakiris and Spiliotis, 2014), the rotational speed of the machines is optimized to minimize the required flow and pressure requirements.

Step B.VI analyzes all scenarios when the design configuration is defined, recalculating the proposed indexes. If any scenario does not meet the predefined constraints, it is identified and re-assessed using the previously established optimization methodology. This iterative process progressively refines the design, ensuring an optimized configuration that fully satisfies system requirements. Finally, as final step, a comprehensive water-energy management assessment is conducted to determine the optimal operational strategy for the system. By analyzing various water-energy performance ratios, it becomes possible to identify the most effective operating points that maximize the distribution volume ratio. This evaluation accounts for both the availability of water volumes and the prevailing irrigation demands, while also incorporating the storage levels of regulation reservoirs across multiple irrigation communities. This approach not only enhances operational efficiency but also reinforces the strategic importance of quantifiable indicators in ensuring sustainable resource management under variable hydrological conditions.

2.2. Case Study

The case study analyzed in this research corresponds to a complex hydraulic system currently facing increasing pressure due to water scarcity, inefficient resource allocation, and the absence of integrated water-energy management strategies by governments (Gómez-Ramos et al., 2024). The traditional operational schemes are no longer sufficient to meet current irrigation demands while ensuring environmental sustainability (Cantos, 2024). In this context, the Zero Discharge methodology emerges as a necessary and innovative approach to optimize the use of available water volumes, minimize uncontrolled discharges, and enhance the overall efficiency of the system. By integrating water-energy interactions and considering the operational constraints of multiple regulation reservoirs, this methodology provides a structured framework to support decision-making under scenarios of growing water stress and climate variability.

The hydraulic system is located in two different cities in the Alicante province, particularly Torrevieja and Orihuela Costa (Figure 4a). It is established for different interlinked subsystems, all converging at a strategic energy-water exchange node: the Villamartín Reservoir (RS02), which operates as a regulation reservoir (Figure 4b).

This multipurpose infrastructure integrates heterogeneous water sources, which are tertiary-treated effluents from wastewater treatment plants (WWTPs), stormwater runoff, and desalinated water. They are distributed by pressurized pipelines by gravity or pumped systems (Figure 4c). The Orihuela Costa subsystem (PS00–PS01–PS08) transports reclaimed water from the local WWTP to storage reservoirs through a photovoltaic pumped system (PVS). The Torrevieja-Torremiguel subsystem (PS02–PS03) captures both waste-treated water and stormwater from the Torrevieja urban area, routing flows through intermediate regulation reservoirs and multiple pumping stages. The main distribution system enables gravitational delivery to multiple irrigation points, while hydraulically interfacing with 'Sumillo' (PS04) and 'Estudiante' (PS05) subsystems. These subsystems incorporate a photovoltaic pumped system to redistribute flows toward downstream areas via gravity, ensuring a low-carbon, energy-resilient

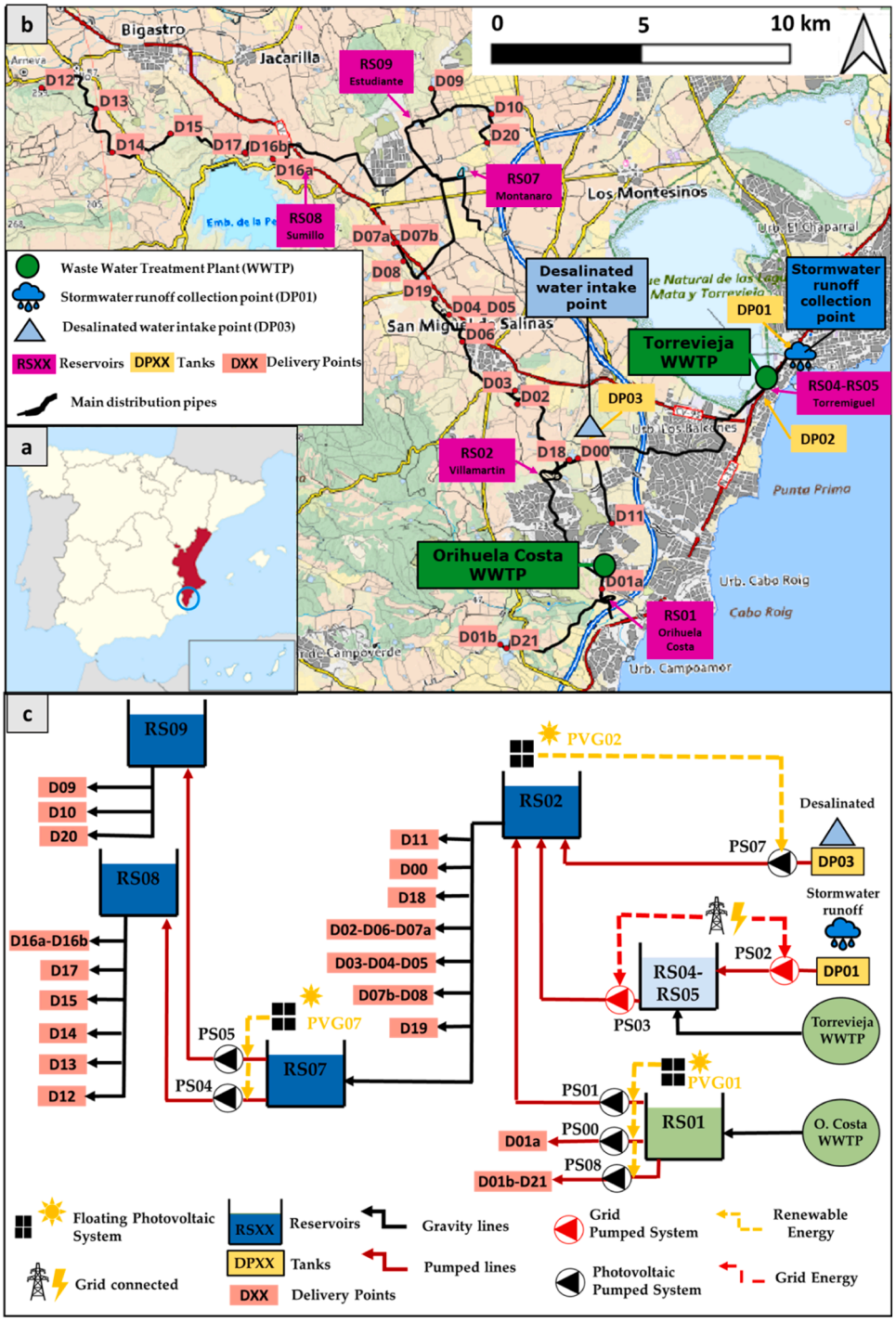

Fig. 4. (a) Case study location; (b) Distribution and location of irrigation points and reservoirs; (c) Hydraulic scheme.

operational profile.

3. RESULTS AND DISCUSSION

3.1. Evaluation of water resources, scenario, and alternatives

The integrated water supply system analyzed in this study comprises four main sources (Figure 5a): the Orihuela Costa WWTP, the Torrevieja WWTP, the Torrevieja desalination plant, and stormwater runoff from the municipality of Torrevieja. Based on historical data, the Orihuela Costa WWTP provides an annual volume of approximately 3.10 hm^3, which could increase up to 4.64 hm^3 in future scenarios. Torrevieja WWTP currently supplies around 7.47 hm^3 annually, with a potential increase to 8.2 hm^3. The desalination plant contributes 2.48 hm^3 annually, considering a future capacity above 3.2 hm^3. Additionally, stormwater runoff is regarded as a complementary source, considering the precipitation in Torrevieja city. The annual contributions range from 0.93 to 1.41 hm^3, depending on the number of rainfall events.

Currently, the wastewater volumes from the Torrevieja WWTP are managed through a 60000 m^3 storage tank, which connects to the PS03. In future configurations, stormwater runoff, which is characterized by high-intensity inflows over short periods, will also be conveyed to the system. This necessitates the expansion of the RS04 reservoir to a minimum total capacity of 310000 m^3 (comprising 250000 m^3 for the future

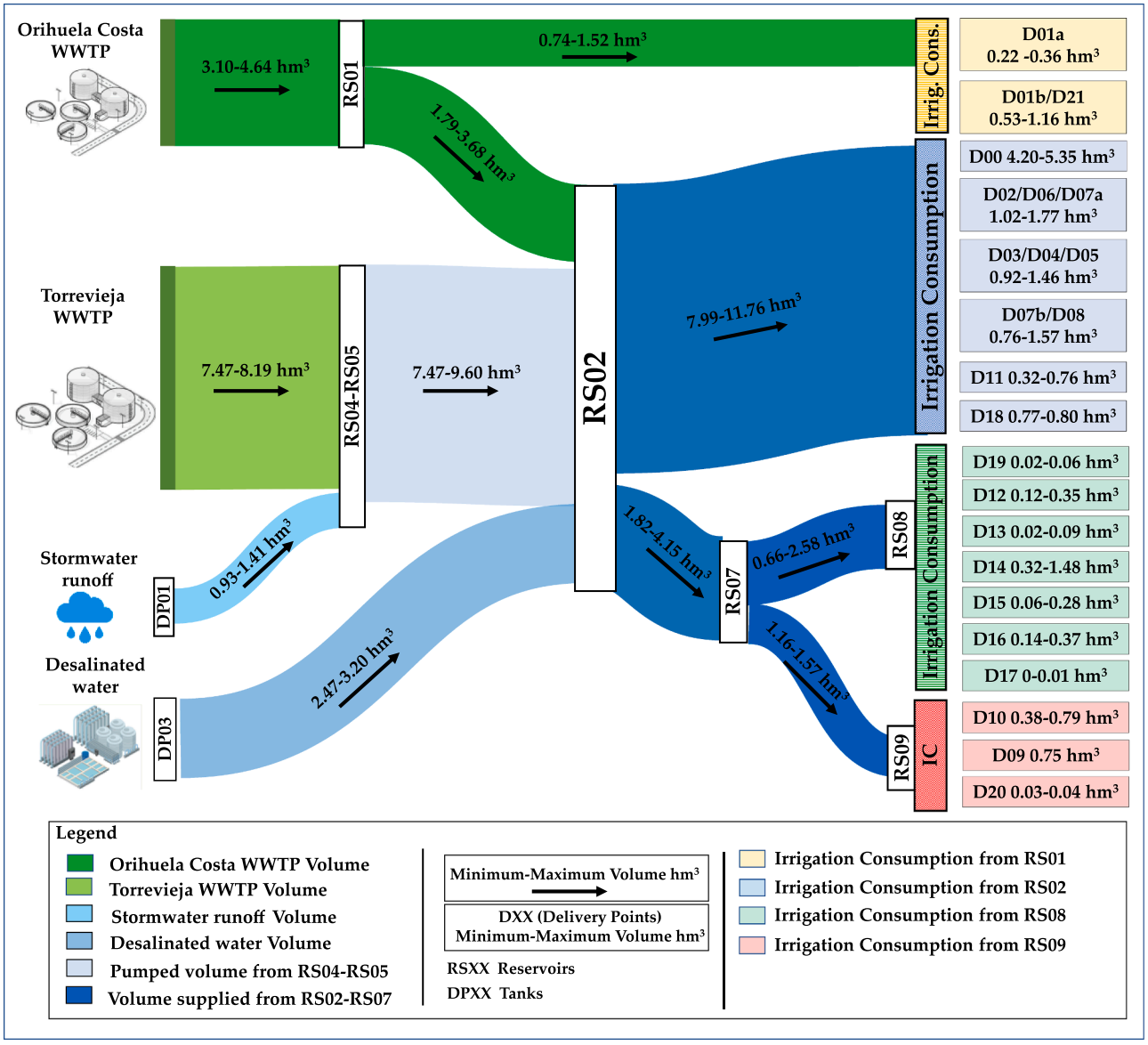

Fig. 5. Distribution of water sources from different resources.

RS05 and 60000 m³ for RS04). This upgrade is essential to ensure effective flow regulation from the WWTP and to accommodate episodic stormwater events before subsequent transfer to RS02. Specifically, 54 scenarios incorporate all inflow hypotheses, including stormwater, and assume a total RS04-RS05 storage capacity of 310000 m³. The generation of these scenarios is critical to capture the variability and complexity of system operation, supporting informed decision-making for resilient and adaptive water infrastructure planning (Figure 6).

Three different alternatives (A1, A2, and A3) were addressed that generated different values of piezometric levels in the reservoirs as well as pumped piezometric levels, resulting from variations in levels and lengths of pipelines. These alternatives were subject to restrictions in terms of layout, protection of natural areas, as well as other types of effects, such as those from municipalities, urban development, and infrastructure. The approach to the alternatives allows for an initial selection of solutions to be made, which can subsequently be used to optimize the design.

3.2. Optimization results

Figure 7a presents the results obtained by evaluating the optimal solutions for each of the three proposed alternatives under different scenarios, using the cost-benefit (B/C) ratio as the objective variable. All other options yield B/C values ranging from 4 to 6.4, with Alternative 1 consistently achieving the highest values, indicating it as the most favourable option.

Figure 7b compares the overall B/C ratios with and without considering the Economic Multiplier Effect (EME). The trend remains consistent, with Alternative 1 still emerging as the most advantageous solution.

In terms of both economic viability and operational indicators (Figures 7c and 7d), Alternative 1 (A1) shows the best results. Figure 7c shows the distribution of the *MRR* over the three alternatives and the 54 scenarios, showing that A1 shows lower values than the other two alternatives. Specifically, it oscillates between values close to 1.4-1.6, while alternative 2 shows oscillations between 1.55 and 1.9 (18.75%

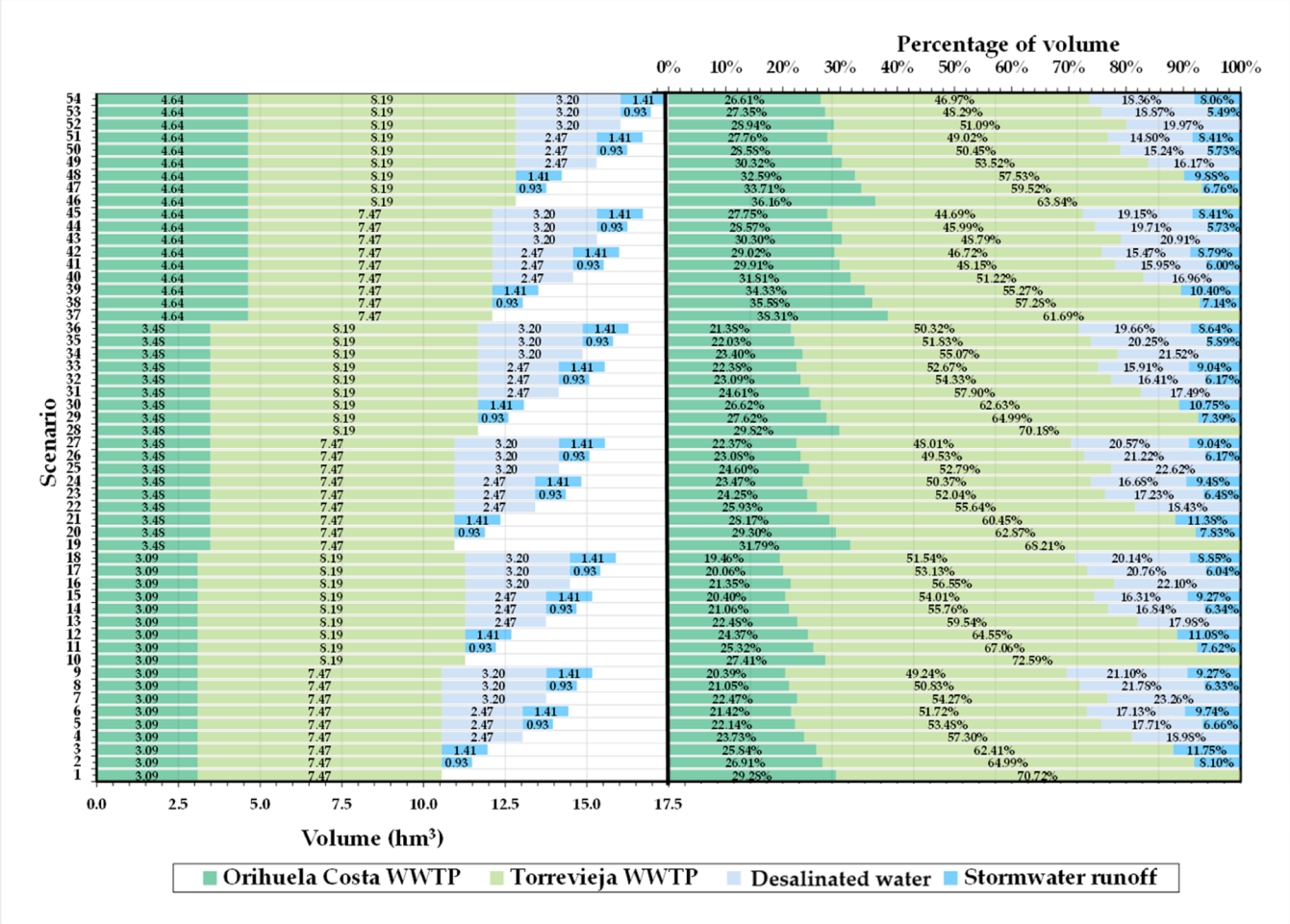

Fig. 6. Evaluation of different scenarios.

higher on average) and alternative 3 shows values between 1.5 and 1.8 (12.5% higher). Figure 7d shows the distribution energy indicator, called *DECR*, showing again the most efficient values in terms of distribution for alternative 1, with average values of 0.45 kWh/m^3, compared to average values of 0.58 and 0.5 kWh/m^3, for alternatives 2 and 3, respectively. Table 2 shows the optimal design results for each alternative (A1, A2, and A3), including maximum pumped flows, reservoir storage capacities, and installed photovoltaic (PV) power required to ensure zero discharge. In general, alternative A2 achieves higher pumped flows in most systems.

For instance, PS01 reaches 0.403 m^3/s in A2 compared to 0.319 m^3/s in A1 and 0.388 m^3/s in A3, while PS07 shows 1.083 m^3/s in A2 versus 0.877 m^3/s in A1 and 1.069 m^3/s in A3. However, this pattern is not consistent across all systems; in PS08, A1 presents a higher value (0.144 m^3/s) compared to A2 (0.101 m^3/s) and A3 (0.100 m^3/s), indicating a more complex system behaviour when evaluated in detail.

Regarding reservoir storage, A3 achieves the highest total capacity at 2.840 hm^3, followed closely by A2 (2.796 hm^3) and A1 (2.495 hm^3). Individual reservoirs exhibit significant variations, such as RS01, where A3 reaches 0.788 hm^3 compared to 0.455 hm^3 and 0.332 hm^3 for A1 and A2, respectively. Conversely, RS02 presents a higher capacity in A2 (1.286 hm^3). As for photovoltaic installations, A2 requires the largest total power (9.75 MW), higher than A1 (6.90 MW) and A3 (8.00 MW), reflecting the additional energy demand linked to its greater pumped flows. Thus, while A2 shows strong individual performance in flow and specific storage, it also incurs greater energy infrastructure requirements.

Although A2 demonstrates advantages in specific pumped flow and reservoir parameters, alternative A1 emerges as a more balanced and efficient solution when considering all design criteria collectively. A1 combines lower photovoltaic power requirements with competitive storage capacities and moderate pumped flows, resulting in a configuration that optimizes infrastructure investment and operational sustainability. Therefore, from a global perspective, A1 provides the most favourable trade-off between hydraulic performance, energy needs, and system resilience.

3.3. *Water management operation*

Figure 8a shows the dynamic behaviour of the system regarding both water volume management under the optimized operational strategy considering the optimal design solution for A1. The annual evolution of moved volume alongside the inlet and outlet flows throughout a representative year. This operational pattern demonstrates the system's ability to effectively buffer inflow fluctuations and optimize reservoir utilization, maintaining water availability while avoiding unnecessary overflows or shortages.

Figure 8b provides a complementary perspective to the water management analysis presented in Figure 8a by detailing the photovoltaic (PV) energy production, the energy consumption associated with the pumping systems, and the resulting energy surplus. The maximum power demand profiles for the principal pumping stations (PS00, PS01, and PS08) reveal that the system's energy requirements consistently remain well below the available PV generation capacity, with demand peaks seldom surpassing 0.45 MW. This energy management behaviour underscores the resilience and effectiveness of the integrated PV-

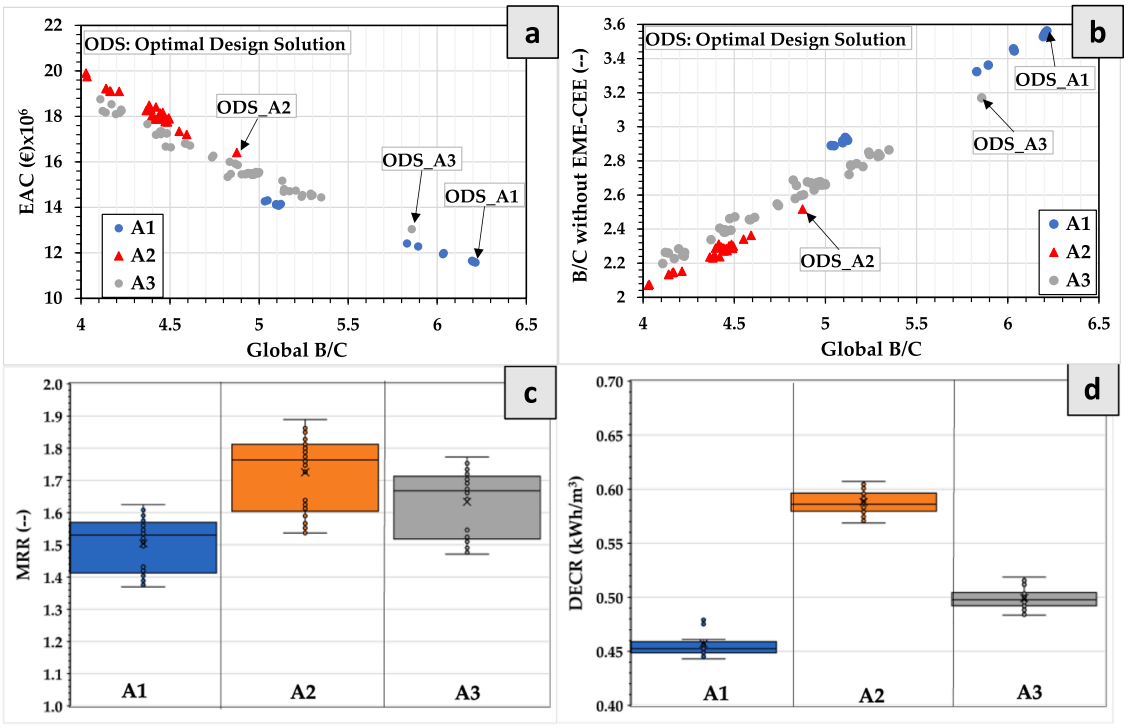

Fig. 7. (a) Global B/C considering the different scenarios and alternatives; (b) Global B/C vs B/C without EME for different alternatives; (c) Manometric Regulation Ratio (MRR) for different optimal solutions for selected scenarios and alternatives; (d) Distributed Energy Consumption Ratio (DECR) for different scenarios.

Table 2
Maximum Pumped Flow, capacity reservoir and installed photovoltaic power for the different optimal design solutions as a function of the alternative.

Maximum Pumped flow (m^3/s)			
Pumped System	A1	A2	A3
PS00	0.053	0.141	0.079
PS01	0.319	0.403	0.388
PS08	0.144	0.101	0.100
PS03	0.387	0.648	0.596
PS04	0.672	0.795	0.761
PS05	0.705	0.898	0.864
PS07	0.877	1.083	1.069
Maximum Capacity of reservoirs (hm^3)			
Reservoir	A1	A2	A3
RS01	0.455	0.332	0.788
RS02	1.035	1.286	1.175
RS04-RS05	0.528	0.560	0.524
RS07	0.062	0.052	0.040
RS08	0.378	0.288	0.270
RS09	0.037	0.278	0.043
Total	2.495	2.796	2.840
Installed photovoltaic power(MW)			
Floating Photovoltaic System	A1	A2	A3
PVG01	3.40	2.25	2.00
PVG02	1.50	3.75	3.00
PVG07	2.00	2.75	3.00
Total	6.90	9.75	8.00

pumped storage configuration, guaranteeing an adequate energy supply even under peak load conditions. The results depicted in Figures 8a and 8b demonstrate the system's capability to integrate hydraulic and photovoltaic resources, thereby achieving stable water management alongside reliable and sustained utilisation of renewable energy over the analysed period. Figure 8c shows the daily behaviour of the system for generated and consumed power as well as the pumped flow of the system, defining the inlet and outlet flow of the different reservoirs, in this case, the RS02.

The global operation and useful for the management of the facility can be observed in Figure 9. Figure 9a shows the different values of capacity ratio in the different reservoirs, which show ranges between 0.4 and 0.68, considering values nearest to 1 in the RS02 and RS04-RS05.

Figure 9b shows the self-consumption ratios of the different photovoltaic systems evaluated. PVG01 presented values between 0.4 and 0.6, while PVG02 stabilized around 0.28. PVG07, composed of two subsystems corresponding to each pumping unit, exhibited a wider range between 0.3 and 0.7. These results were consistent with previous studies, which highlighted that photovoltaic self-consumption largely depended on system configuration and the alignment between generation and demand profiles (Luthander et al., 2015). In scenarios with excess energy, the possibility of injecting it into the wastewater treatment plants (WWTPs) was considered to further improve energy integration.

The Distribution Volume Ratio (DVR) emerged as a key performance indicator to ensure both proper system operation and the goal of zero wastewater discharge to the sea, in line with the principles of circular water management (Larsen et al., 2016). Figure 9c illustrated a sensitivity analysis of the DVR under variations in wastewater volumes generated at the WWTPs, based on the optimized configuration of Alternative A1. The system demonstrated robust behavior, maintaining DVR values above 0.9 in all scenarios. Full circularity (DVR = 1) was achieved for volumes below 5.25 hm^3 in Orihuela Costa and 9.5 hm^3 in Torrevieja. As inflows increased, a controlled and gradual reduction in DVR was observed, highlighting the system's resilience under variable conditions (Hinegk et al., 2022).

Figure 9d evaluated the system's adaptability to reductions in the generated power of the PVG01 and PVG07 units. Despite the decrease in energy input, the system maintained its operational effectiveness, confirming the suitability of the integrated energy-water management approach (Fan et al., 2021). Overall, the proposed methodology provided a replicable framework to improve water reuse efficiency, enhance operational flexibility, and support sustainable resource

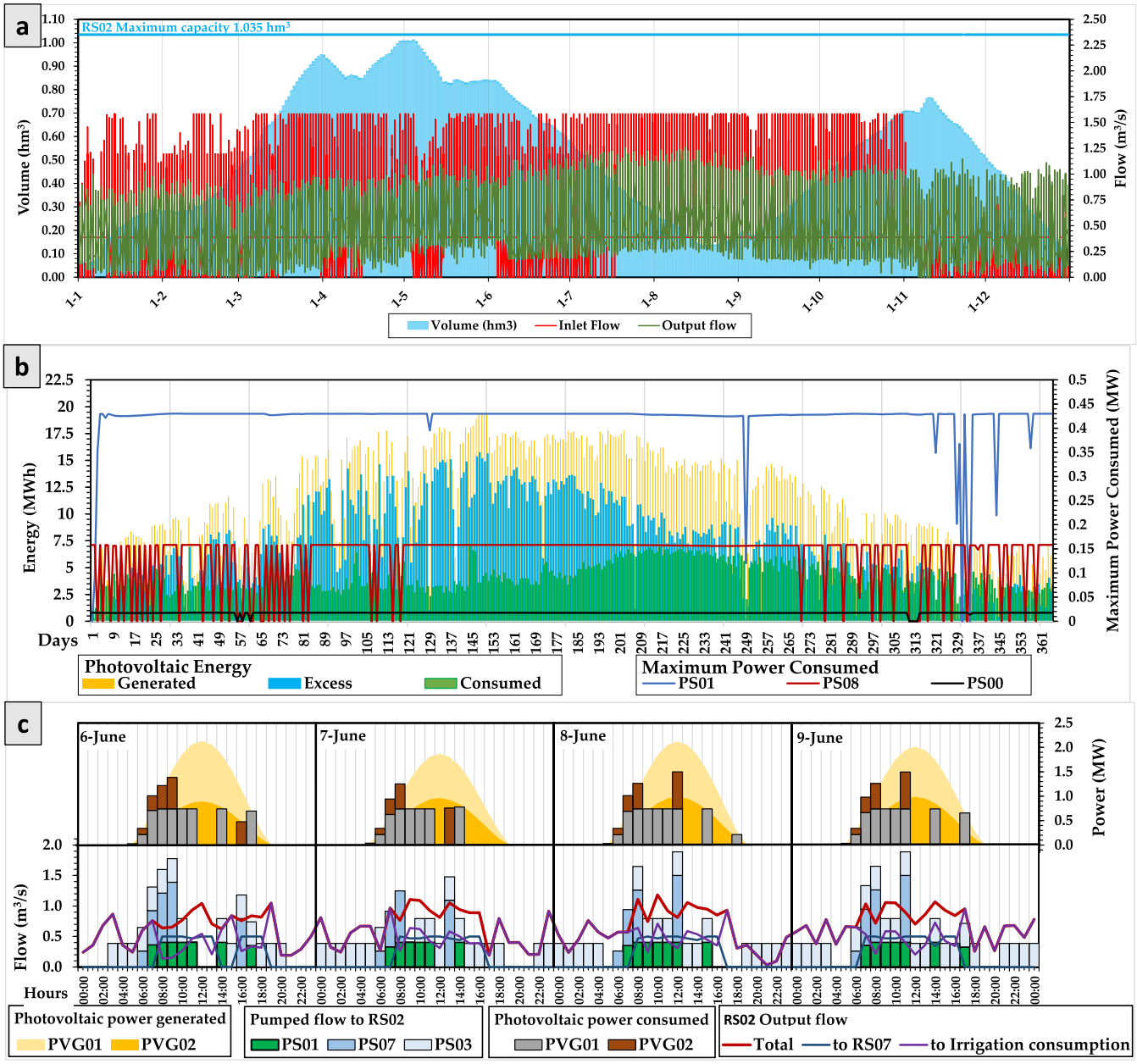

Fig. 8. (a) Transferred Volume, input and output flows in RS02; (b) Evaluation of the balance in photovoltaic energy and maximum power consumed in the different pumped systems; (c) Daily power and flow details. All Fig.s are established for scenario number 54.

management in urban water systems (Garcia and Pargament, 2015).

Figure 10a establishes the optimal designed solution, the *DC* variation ranging from 1.1 to 0.7 when the *SVI* changed in the facilities. It is inverse to *B/C without CEE*, which when the *DC* is 1.1, the *B/C without CEE* is above 5, while it increase above 1 when the *DC* is minimum for *SVI* equal to 1.7. This values are aligned with the established by (Suresh Kumar, 2016), which defined values between 0.9 and 2 when the CEE is not considered. This trend suggests that more sustainable hydraulic alternatives may require higher upfront investments, potentially lowering their immediate economic profitability if externalities are not properly valued. This aligns with previous studies highlighting the need to integrate environmental and social co-benefits in cost-benefit assessments to avoid underestimating sustainable solutions (Zhang et al., 2021).

Figure 10b illustrates the variation in *UGPR* values as the *SVI* ranged from 1.05 to 1.6. During this interval, the *UGPR* decreased from 0.65 to 0.4, indicating a declining trend in potential performance. This suggests that under high-SVI configurations of renewable power generation may exceed the system's real-time energy demand, reducing the effectiveness of direct energy usage. This behavior is consistent with findings in the water-energy nexus literature, where mismatches between renewable generation profiles and hydraulic demand curves limit system-wide performance without adequate storage or smart controls (Parajuli et al., 2023). In this case, the topography of the area did not enable the use of potential water reservoir to incorporate a pumped hydro-storage system to improve self-consumption, reducing the installed photovoltaic power systems (Naval et al., 2023).

4. CONCLUSION

This study presents a hybrid volume regulation framework that integrates reclaimed water, stormwater runoff, and desalinated water, demonstrating high operational performance and resilience under variable hydrological and energy conditions. Developed under quasi-steady assumptions, the system emphasizes flexibility to adapt to fluctuating

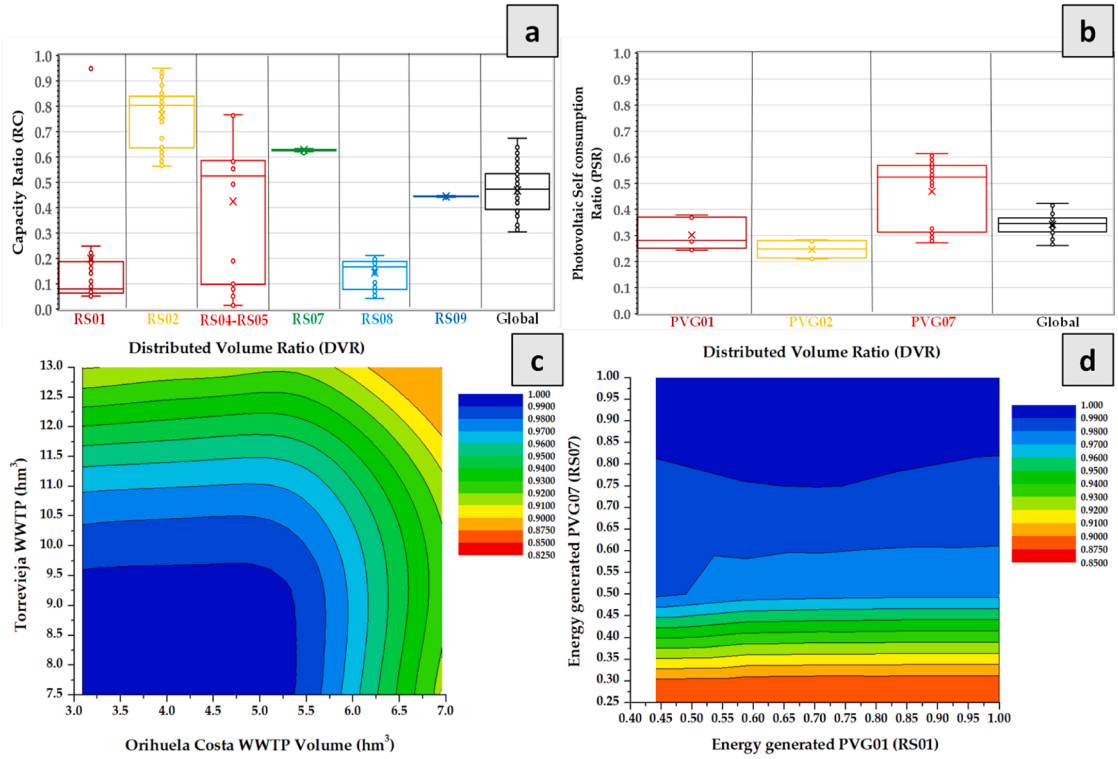

Fig. 9. (a) Capacity ratio for the different reservoirs; (b) Self-Consumption Photovoltaic Ratio for the different PV systems; (c) Distributed Volume Ratio (DVR) as a function of generated water volume of the WWTPs; (d) Distributed Volume Ratio (DVR) as a function of generated energy of the PV systems.

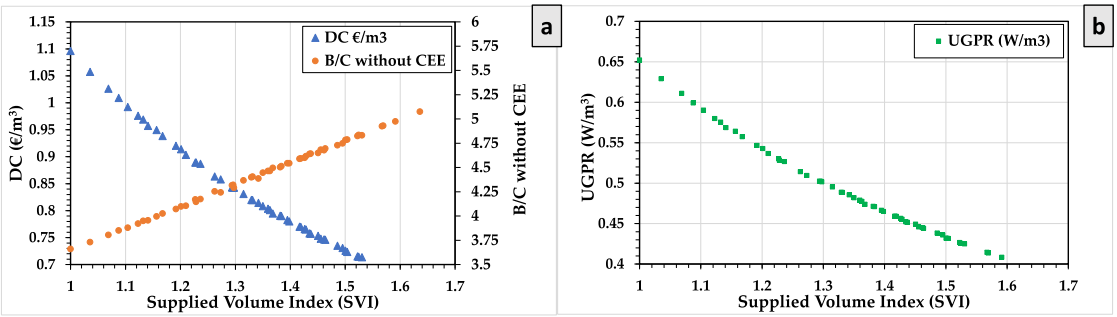

Fig. 10. (a) Distribution Cost (DC) and B/C without CEE as a function of the SVI. (b) Used Generated Power Ratio (UPGR) as a function of SVI.

solar radiation, inflows, and demand. Scenario-based analysis of 54 scenarios confirms the robustness of the design, with *CR* values above 0.7, allocation ratios exceeding 0.965, and *DVR* values typically above 0.975. The *SVI* further evidences efficient distribution within an integrated water resource management context, evaluating the *DC* and *B/C*.

The incorporation of photovoltaic-powered pumping, combined with sensitivity analyses for flow and capacity calibration, ensures energy-efficient operation even under adverse conditions. The system effectively absorbs demand redistribution during non-consumptive periods, and design enhancements such as optimizing desalinated water injection points can further reduce energy use and investment costs. Overall, the methodology offers a scalable and transferable strategy for advancing hybrid water-energy systems, supporting climate-resilient infrastructure and zero-discharge objectives. Future work should address model limitations, such as the quasi-steady assumption, and explore real-time control strategies, extended monitoring under diverse climatic regimes, integration of the evaluation of quality mixed water, and integration with emerging storage technologies to further validate and enhance system applicability.

Funding

Funding for open access charge: CRUE-Universitat Politècnica de València

CRediT authorship contribution statement

Miguel-Ángel Bofill: Investigation, Formal analysis. **Francisco-Javier Sánchez-Romero:** Writing – original draft, Methodology, Conceptualization. **Francisco A. Zapata:** Supervision. **Helena M. Ramos:** Writing – review & editing, Validation. **Modesto Pérez-Sánchez:** Writing – original draft, Supervision, Resources, Methodology, Conceptualization.

Declaration of competing interest

The authors declare that they have no known competing financial interests or personal relationships that could have appeared to influence the work reported in this paper.

ACKNOWLEDGMENT

The authors are grateful for the project HY4RES (Hybrid Solutions for Renewable Energy 962 Systems) EAPA_0001/2022 from INTERREG ATLANTIC AREA PROGRAMME. This research was supported by the project DAFNE – Optimization to Promote, Improve, and Increase the Efficiency of Water Resource Management for Integration into Irrigation Systems (AEST/2023/82), funded by the Conselleria d'Educació, Investigació, Cultura i Esport de la Generalitat Valenciana.

Data availability

Data will be made available on request.

References

Ávila, C.A.M., Sánchez-Romero, F.J., López-Jiménez, P.A., Pérez-Sánchez, M., 2021. Leakage management and pipe system efficiency. Its influence in the improvement of the efficiency indexes. Water 13, 1909. https://doi.org/10.3390/W13141909, 2021, Vol. 13, Page 1909.

Ahluwalia, O., Singh, P.C., Bhatia, R., 2021. A review on drought stress in plants: implications, mitigation and the role of plant growth promoting rhizobacteria. Resour. Environ. Sustain. 5, 100032. https://doi.org/10.1016/J.RESENV.2021.100032.

Al Hamedi, F.H., Kandhan, K., Liu, Y., Ren, M., Jaleel, A., Alyafei, M.A.M, 2023. Wastewater irrigation: a promising way for future sustainable agriculture and food security in the United Arab Emirates. Water 15, 1–18. https://doi.org/10.3390/w15122284.

Alimentación, M.de A.P.y ESPAÑOLA A TRAVÉS DEL ANÁLISIS DEL CENSO AGRARIO 2020 informe de análisis; 2023.

Alyssa Ahmad Affandi, N., Ahmad Ludin, N., Mukminah Junedi, M., Chin Haw, L., Purvis-Roberts, K., 2024. Analysing temporal factor in dynamic life cycle assessment of solar photovoltaic system. Sol. Energy 270, 112380. https://doi.org/10.1016/J.SOLENER.2024.112380.

Anjum, R., Parvin, F., Ali, S.A., 2023. Machine learning applications in sustainable water resource management: a systematic review. Springer Water 29–47. https://doi.org/10.1007/978-3-031-35279-9_2/TABLES/1. Part F1186.

Anser, M.K., Yousaf, S.U., Usman, B., Azam, K., Bandar, N.F.A., Jambari, H., Sriyanto, S., Zaman, K., 2023. Beyond climate change: examining the role of environmental justice, agricultural mechanization, and social expenditures in alleviating rural poverty. Sustain. Futur. 6, 100130. https://doi.org/10.1016/j.sftr.2023.100130.

Bernardo, M.G.; Belén, G.E.; Victoriano, M.Á.; José Francisco, M.V. Balance de carbono de las zonas regables del trasvase Tajo-Segura; 2020.

Borrego-Marín, M.M., Berbel, J., 2019. Cost-benefit analysis of irrigation modernization in Guadalquivir River Basin. Agric. Water Manag. 212, 416–423. https://doi.org/10.1016/J.AGWAT.2018.08.032.

Cantos, J.O., 2024. Water planning and management in Spain in a climate change context: facts and proposals. Geogr. Res. Lett. 50, 3–28. https://doi.org/10.18172/CIG.6453.

Christou, A., Beretsou, V.G., Iakovides, I.C., Karaolia, P., Michael, C., Benmarhnia, T., Chefetz, B., Donner, E., Gawlik, B.M., Lee, Y., et al., 2024. Sustainable wastewater reuse for agriculture. Nat. Rev. Earth Environ. 57 (5), 504–521. https://doi.org/10.1038/s43017-024-00560-y, 2024.

Cost, T.H.E.; Action, O.F.; Cost, T.H.E.; No, O.F. Economic valuation of wastewater; 2016; ISBN 9789280734744.

del Villar, A., García-López, M., 2023. The potential of wastewater reuse and the role of economic valuation in the pursuit of sustainability: the case of the Canal de Isabel II. Sustain. 15. https://doi.org/10.3390/su15010843.

Dotaniya, M.L., Meena, V.D., Saha, J.K., Dotaniya, C.K., Mahmoud, A.E.D., Meena, B.L., Meena, M.D., Sanwal, R.C., Meena, R.S., Doutaniya, R.K., et al., 2023. Reuse of Poor-Quality Water For Sustainable Crop Production in the Changing Scenario of Climate. Springer, Netherlands, p. 25. ISBN 0123456789.

Eekhout, J.P.C., Delsman, I., Baartman, J.E.M., van Eupen, M., van Haren, C., Contreras, S., Martínez-López, J., de Vente, J., 2024. How future changes in irrigation water supply and demand affect water security in a Mediterranean catchment. Agric. Water Manag. 297, 108818. https://doi.org/10.1016/j.agwat.2024.108818.

Electrica, R. La demanda de energía electrica en España; 2002.

Elseify, M.A., Hashim, F.A., Hussien, A.G., Kamel, S., 2024. Single and multi-objectives based on an improved golden jackal optimization algorithm for simultaneous integration of multiple capacitors and multi-type DGs in distribution systems. Appl. Energy 353, 122054. https://doi.org/10.1016/J.APENERGY.2023.122054.

Eshtawi, T., Evers, M., Tischbein, B., Diekkrüger, B., 2016. Integrated hydrologic modeling as a key for sustainable urban water resources planning. Water Res. 101, 411–428. https://doi.org/10.1016/J.WATRES.2016.05.061.

Estévez, S., Arias, A., Feijoo, G., Moreira, M.T., 2025. Methodological guide and roadmap to assess the compliance of wastewater treatment plants with sustainability and circularity criteria. Water Res. 274, 123125. https://doi.org/10.1016/J.WATRES.2025.123125.

Estrela-Segrelles, C., Pérez-Martín, M.Á., Wang, Q.J., 2024. Adapting water resources management to climate change in water-stressed River basins—Júcar River Basin case. Water 16. https://doi.org/10.3390/w16071004.

Expósito, A., Berbel, J., 2017. Agricultural irrigation water use in a closed Basin and the impacts on water productivity: the case of the Guadalquivir River Basin (southern Spain. Water (Basel) 9, 136. https://doi.org/10.3390/W9020136, 2017VolPage9136.

Fan, D., Sun, H., Yao, J., Zhang, K., Yan, X., Sun, Z., 2021. Well production forecasting based on ARIMA-LSTM model considering manual operations. Energy 220, 119708. https://doi.org/10.1016/J.ENERGY.2020.119708.

Fu, G., Jin, Y., Sun, S., Yuan, Z., Butler, D., 2022. The role of deep learning in urban water management: a critical review. Water Res 223, 118973. https://doi.org/10.1016/J.WATRES.2022.118973.

Gómez-Ramos, A., Blanco-Gutiérrez, I., Ballesteros-Olza, M., Esteve, P., 2024. Are non-conventional water resources the solution for the structural water deficit in Mediterranean agriculture? The case of the Segura River Basin in Spain. Water 16, 929. https://doi.org/10.3390/W16070929, 2024, Vol. 16, Page 929.

García-Ruiz, J.M., López-Moreno, J.I., Vicente-Serrano, S.M., Lasanta–Martínez, T., Beguería, S., 2011. Mediterranean water resources in a global change scenario. Earth-Science Rev 105, 121–139. https://doi.org/10.1016/j.earscirev.2011.01.006.

Garcia, X., Pargament, D., 2015. Reusing wastewater to cope with water scarcity: economic, social and environmental considerations for decision-making. Resour. Conserv. Recycl. 101, 154–166. https://doi.org/10.1016/J.RESCONREC.2015.05.015.

Garcia, C., López-Jiménez, P.A., Sánchez-Romero, F.J., Pérez-Sánchez, M., 2023. Assessing water urban systems to the compliance of SDGs through sustainability indicators. Implementation in the valencian community. Sustain. Cities Soc. 96, 104704. https://doi.org/10.1016/J.SCS.2023.104704.

Guerra-Rodríguez, S., Oulego, P., Rodríguez, E., Singh, D.N., Rodríguez-Chueca, J., 2020. Towards the implementation of circular economy in the wastewater sector: challenges and opportunities. Water 12. https://doi.org/10.3390/w12051431.

Hinegk, L., Adami, L., Zolezzi, G., Tubino, M., 2022. Implications of water resources management on the long-term regime of Lake Garda (Italy). J. Environ. Manage. 301, 113893. https://doi.org/10.1016/J.JENVMAN.2021.113893.

Hui, C.X., Dan, G., Alamri, S., Toghraie, D., 2023. Greening smart cities: an investigation of the integration of urban natural resources and smart city technologies for promoting environmental sustainability. Sustain. Cities Soc. 99, 104985. https://doi.org/10.1016/j.scs.2023.104985.

Joseph, K., Sharma, A.K., van Staden, R., Wasantha, P.L.P., Cotton, J., Small, S., 2023. Application of software and hardware-based technologies in leaks and burst detection in water pipe networks: a literature review. Water 15.

Koop, S.H.A., Grison, C., Eisenreich, S.J., Hofman, J., van Leeuwen, K.J., 2022. Integrated water resources management in cities in the world: global solutions. Sustain. Cities Soc. 86. https://doi.org/10.1016/j.scs.2022.104137.

Larsen, T.A., Hoffmann, S., Lüthi, C., Truffer, B., Maurer, M., 2016. Emerging solutions to the water challenges of an urbanizing world. Science 352, 928–933. https://doi.org/10.1126/SCIENCE.AAD8641/ASSET/A9922F96-BEE1-463A-87D3-ACA9AE961B79/ASSETS/GRAPHIC/352_928_T2D.JPEG.

Liang, D., Lu, H., Guan, Y., Feng, L., Chen, Y., He, L., 2023. Further mitigating carbon footprint pressure in urban agglomeration by enhancing the spatial clustering. J. Environ. Manage. 326. https://doi.org/10.1016/j.jenvman.2022.116715.

Luthander, R., Widén, J., Nilsson, D., Palm, J., 2015. Photovoltaic self-consumption in buildings: a review. Appl. Energy 142, 80–94. https://doi.org/10.1016/J.APENERGY.2014.12.028.

Shengsong Mei; Zhuo Huang; Kangling Fang A neural network controller based on genetic algorithms. 2002, 1624–1628, doi:10.1109/ICIPS.1997.669316.

Mercedes Garcia, A.V., Sánchez-Romero, F.J., López-Jiménez, P.A., Pérez-Sánchez, M., 2022. A new optimization approach for the use of hybrid renewable systems in the search of the zero net energy consumption in water irrigation systems. Renew. Energy 195, 853–871. https://doi.org/10.1016/J.RENENE.2022.06.060.

Metcalf, G.E.; Stock, J.H. Integrated assessment models and the social cost of carbon: a review and assessment of U.S. Experience. https://doi.org/10.1093/reep/rew014 2017, 11, 80–99.

Migo-Sumagang, M.V., Tan, R.R., Aviso, K.B., 2023. A multi-period model for optimizing negative emission technology portfolios with economic and carbon value discount rates. Energy 275, 127445. https://doi.org/10.1016/J.ENERGY.2023.127445.

Mishra, S., Kumar, R., Kumar, M., 2023. Use of treated sewage or wastewater as an irrigation water for agricultural purposes- environmental, health, and economic impacts. Total Environ. Res. Themes 6, 100051. https://doi.org/10.1016/J.TOTERT.2023.100051.

Molinos-Senante, M., Hernández-Sancho, F., Sala-Garrido, R., 2011. Cost–benefit analysis of water-reuse projects for environmental purposes: a case study for Spanish wastewater treatment plants. J. Environ. Manage. 92, 3091–3097. https://doi.org/10.1016/j.jenvman.2011.07.023.

Naval, N., Yusta, J.M., Sánchez, R., Sebastián, F., 2023. Optimal scheduling and management of pumped hydro storage integrated with grid-connected renewable power plants. J. Energy Storage 73, 108993. https://doi.org/10.1016/J.EST.2023.108993.

Nishanth, J.R., Kushwaha, K.K., Deshmukh, M.A., Balaji, S., Kushwah, R., Sampath, B., 2023. Particle swarm optimization of hybrid renewable energy systems. Intelligent Engineering Applications and Applied Sciences for Sustainability, 1AD, pp. 291–308. https://doi.org/10.4018/979-8-3693-0044-2.ch016.

Oğuz, A., Ertuğrul, Ö.F., 2023. A survey on applications of machine learning algorithms in water quality assessment and water supply and management. Water Suppl. 23, 895–922. https://doi.org/10.2166/WS.2023.033.

Parajuli, S., Narayan Bhattarai, T., Gorjian, S., Vithanage, M., Raj Paudel, S., 2023. Assessment of potential renewable energy alternatives for a typical greenhouse aquaponics in Himalayan Region of Nepal. Appl. Energy 344, 121270. https://doi.org/10.1016/J.APENERGY.2023.121270.

Pedrero, F., Kalavrouziotis, I., Alarcón, J.J., Koukoulakis, P., Asano, T., 2010. Use of treated municipal wastewater in irrigated agriculture—Review of some practices in Spain and Greece. Agric. Water Manag. 97, 1233–1241. https://doi.org/10.1016/J.AGWAT.2010.03.003.

Qadir, M.; Jones, E. Domestic wastewater generation, treatment, and agricultural reuse. 2024.

Quinn, N.W.T., Brekke, L.D., Miller, N.L., Heinzer, T., Hidalgo, H., Dracup, J.A., 2004. Model integration for assessing future hydroclimate impacts on water resources, agricultural production and environmental quality in the San Joaquin Basin, California. Environ. Model. Softw 19, 305–316. https://doi.org/10.1016/S1364-8152(03)00155-5.

Ríos, I.H., Cruz-Pérez, N., Chirivella-Guerra, J.I., García-Gil, A., Rodríguez-Alcántara, J. S., Rodríguez-Martín, J., Marazuela, M.Á., Santamarta, J.C., 2023. Proposed recharge of island aquifer by deep wells with regenerated water in Gran Canaria (Spain). Groundw. Sustain. Dev. 22, 100959. https://doi.org/10.1016/j.gsd.2023.100959.

Ramos, A.F., Santos, F.L., 2010. Yield and olive oil characteristics of a low-density orchard (cv. Cordovil) subjected to different irrigation regimes. Agric. Water Manag. 97, 363–373. https://doi.org/10.1016/J.AGWAT.2009.10.008.

Segura, C.H. del Sostenibilidad de los regadíos del Tajo-Segura; 2021.

Serra-Wittling, C., Molle, B., Cheviron, B., 2019. Plot level assessment of irrigation water savings due to the shift from sprinkler to localized irrigation systems or to the use of soil hydric status probes. Application in the French context. Agric. Water Manag 223, 105682. https://doi.org/10.1016/j.agwat.2019.06.017.

Sheet, E.P.A.F, 2016. Social cost of carbon. High. Educ. Whisperer 1–5.

Sindicato Central de Regantes del Acueducto, 2020. Tajo-Segura Impacto económico del trasvase Tajo-Segura en Alicante. Almería y Murcia.

Su, C., Madani, H., Liu, H., Wang, R., Palm, B., 2020. Seawater heat pumps in China, a spatial analysis. Energy Convers. Manag. 203, 112240. https://doi.org/10.1016/j.enconman.2019.112240.

Suresh Kumar, D. Social benefit cost analysis of drip irrigation. 2016, 113–131, doi:10.1007/978-981-10-0348-6_7.

Trapote, A., Albaladejo, A., Simón, P., 2014. Energy consumption in an urban wastewater treatment plant: the case of Murcia Region (Spain). Civ. Eng. Environ. Syst. 31, 304–310. https://doi.org/10.1080/10286608.2013.866106.

Tsakiris, G., Spiliotis, M., 2014. A Newton–Raphson analysis of urban water systems based on nodal head-driven outflow. Eur. J. Environ. Civ. Eng. 18, 882–896. https://doi.org/10.1080/19648189.2014.909746.

Wang, S., Taha, A.F., Abokifa, A.A., 2021. How effective is model predictive control in real-time water quality regulation? State-space modeling and scalable control. Water Resour. Res 57, e2020WR027771. https://doi.org/10.1029/2020WR027771.

Wang, Y., Zhang, Y., Wang, W., Liu, Z., Yu, X., Li, H., Wang, W., Hu, X., 2023. A review of optimal design for large-scale micro-irrigation pipe network systems. Agronomy 13.

Wu, Z.Y., Chew, A., Meng, X., Cai, J., Pok, J., Kalfarisi, R., Lai, K.C., Hew, S.F., Wong, J. J., 2023. High Fidelity digital twin-based anomaly detection and localization for smart water grid operation management. Sustain. Cities Soc 91, 104446. https://doi.org/10.1016/J.SCS.2023.104446.

Xiang, X., Li, Q., Khan, S., Khalaf, O.I., 2021. Urban water resource management for sustainable environment planning using artificial intelligence techniques. Environ. Impact Assess. Rev. 86, 106515. https://doi.org/10.1016/J.EIAR.2020.106515.

Zhan, C., Tian, M., Liu, Y., Zhou, J., Yi, X., 2022. A novel greedy adaptive ant colony algorithm for shortest path of irrigation groups. Math. Biosci. Eng. 19, 9018–9038. https://doi.org/10.3934/mbe.2022419.

Zhang, Y., Li, X., Šimůnek, J., Shi, H., Chen, N., Hu, Q., Tian, T., 2021. Evaluating soil salt dynamics in a field drip-irrigated with brackish water and leached with freshwater during different crop growth stages. Agric. Water Manag. 244, 106601. https://doi.org/10.1016/J.AGWAT.2020.106601.